

A Gaussian Fitter for the CESR-c Fast Luminosity Monitor

Katherine L. Dooley*

Vassar College, Poughkeepsie, New York 12604 USA

(Dated: July 21, 2004)

The purpose of the CESR-c fast luminosity monitor (FLM) is to count the rate of photons emitted from radiative bhabha events at the interaction point. Instantaneous luminosity can thus be determined which will guide the CESR operator in optimizing the accelerator. We wrote a χ^2 minimization program for a Gaussian function to account for all photons, including those that do not strike the monitor's window. Testing the fitter with data representing the range of possible beam parameters and additional noise, we find that the algorithm works well to produce a 1% statistical measurement of luminosity.

I. INTRODUCTION

Recently, an initiative to incorporate a fast luminosity monitor into Cornell's particle accelerator at Wilson Lab has been approved. Much effort is being put forth towards its design, construction, and testing. This monitor will measure the rate at which photons are emitted from radiative bhabha events at the interaction point. Ultimately, the FLM will provide a reliable means of collecting data to calculate the instantaneous luminosity at the interaction point. In order for luminosity to be determined, the data must first be analyzed with the aid of a computer program. By measuring the luminosity, we can determine the number of interesting physics events in CLEO. The CESR operator can use this timely information to find the best machine parameters in order to maximize luminosity. Past experience suggests that three times improvement in luminosity is obtained through careful tuning of initial design conditions. Significant reduction in luminosity maintenance time is also expected.

First, I will present some background information about luminosity and discuss the basic design and theory of the fast luminosity monitor. Then, I will show that such a detector really is feasible. A description of my program which finds the best fit Gaussian curve for the FLM data will be followed by a presentation of results. Uncertainties and ideas for future work will come last.

II. LUMINOSITY

When an electron and positron collide at CLEO, an array of sub-atomic particles is produced. The specific emission, however, depends on the type of interaction. A common interaction is the radiative bhabha event, an inelastic collision between the electron and positron. The energy loss from this type of event is used to produce a photon. Luminosity can be determined by measuring the rate at which these photons are emitted.

*kadooley@vassar.edu

The rate R of the radiative bhabha events is related to the luminosity L at the interaction point by the equation

$$R = \sigma L. \quad (1)$$

Here, σ is the cross-section for the radiative bhabha process and has a well defined value. R , however, cannot be precisely known as it is different from the observed rate which is equal to R times an acceptance and efficiency factor. Consequently, we have that

$$L \propto R(\text{RB}) \quad (2)$$

where RB stands for radiative bhabha.

III. PHOTON BEAM

The radiative bhabha photons are emitted in the direction of the positron beam at the interaction point. The angular distribution of the beam is characterized by a typical $1/\gamma$ cone. With CESR operating at 1.88 GeV per beam, one expects most of the photons to be emitted within a cone of 0.27 mrad around the positron beam direction. However, it is the divergence of the positron beam itself that plays a more integral role in determining the shape of the photon beam. The horizontal divergence is controlled quite well by the hardware of the accelerator and remains at 0.65 mrad. More difficulties arise with maintaining the vertical divergence, and this will typically range from anywhere between 0.47 to 0.82 mrad. Given that

$$\theta_{total} \approx \sqrt{\theta_{\gamma}^2 + \theta_{beam}^2} \quad (3)$$

where θ represents divergence, and using the mean values for θ_{γ} and θ_{beam} , we see that $\theta_{total}=0.66$ mrad. Thus, it is the positron beam divergence at the interaction point that plays the predominate role in determining the divergence of the photon beam.

This divergence is critical as the spot size at the detector depends on it. The photons exit the vacuum chamber 16.1 m away from the interaction point. At this distance and with the beam energy of 1.88 GeV, one standard deviation of the horizontal spot size will be 1.05 cm. In the vertical direction, one standard deviation of the spot size will typically range from 0.76 to 1.32 cm.

IV. THE DETECTOR

The detector itself, which will be placed 16.1 m to the west of the interaction point, is made up of three main components: an aluminum window, scintillators, and photomultiplier tubes. Six plastic scintillators placed 1.1 cm apart make up the vertical portion of the readout. These are placed behind the rectangular window which is 5.08 cm tall and 11.05 cm wide. The window is a one inch thick piece of aluminum. The six scintillators are connected to light guides which connect to photomultiplier tubes, one for each scintillator. (See Fig. 1).

The incoming high energy photons first strike the aluminum window. Here, pair production occurs as the photons enter the electric fields surrounding the nuclei of the high Z aluminum atoms where Z is the charge on the nucleus. During this process, the initial intensity I_0 of the photon beam is reduced by a factor of e to I where

$$I = I_0 \exp\left(-\frac{7x}{9X_0}\right). \quad (4)$$

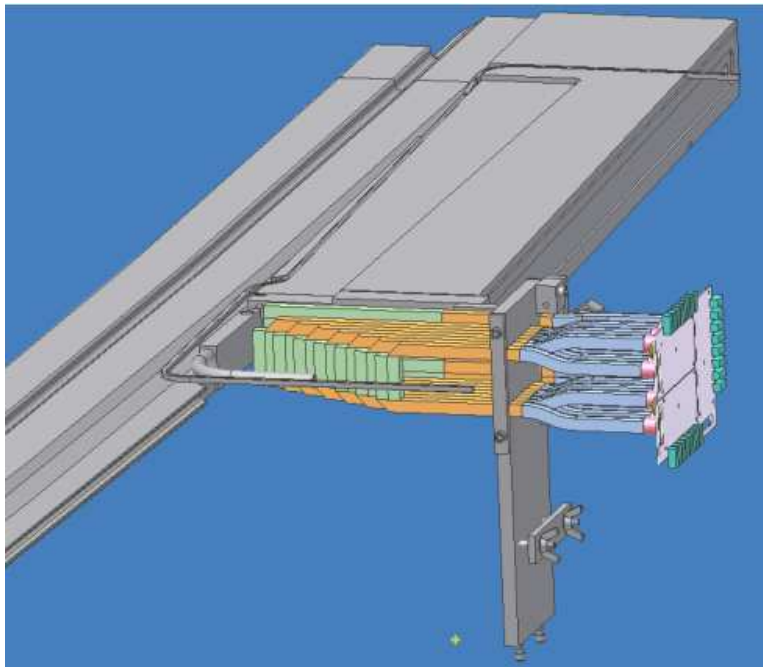


FIG. 1: A drawing of the proposed fast luminosity monitor. Green segments are the scintillators and blue segments are light guides leading to the photomultiplier tubes. The detector is mounted on the vacuum chamber.

One radiation length is given by X_0 which describes the distance needed in a given material for a photon to pair produce [?]. The aluminum is 0.26 radiation lengths thick. This means that about 20% of the photons will actually convert.

Typically, either two or four electrons and positrons exit the aluminum and enter the scintillators where molecules are excited. When the electrons of the molecules fall back to their ground state, a visible photon is emitted. Upon passing through light guides, these photons then strike the photocathode of the photomultiplier tube where they emit electrons via the photoelectric effect. After passing through a series of anodes, each electron is multiplied by a factor of about $10^4 - 10^6$. This is read out from the photomultiplier tubes as a current.

Before constructing and implementing the detector, we must confirm that it will work well and meet the needs of the project. Here, we will perform a simple calculation to estimate an expected output current and then compare that to the photomultiplier tube specifications. First, we assume that due to the geometry of the situation, half of the photons emitted from the scintillator will reach the photomultiplier tubes. Then, for every 100 MeV of energy, one photon will be produced in the scintillators [?]. We project that the photomultiplier tube will be 10% efficient in creating electrons and that it has a gain factor of 10^6 electrons.

The only other necessary piece of information to calculate the current is a value for the photon energy density per unit time at the fast luminosity monitor. We get this from a GEANT simulation as seen in Fig. 2. Using a peak value of 1.9×10^{11} eV/cm³/s, current is approximately 9 μ A.

The Hamamatsu R7400U photomultiplier tube functions with currents up to 13 μ A. The 9 μ A we expect is well within that range. Furthermore, as seen in Fig. 3, a gain of 10^5 is in the middle of the R7400's operating range. This is important as one can easily provide

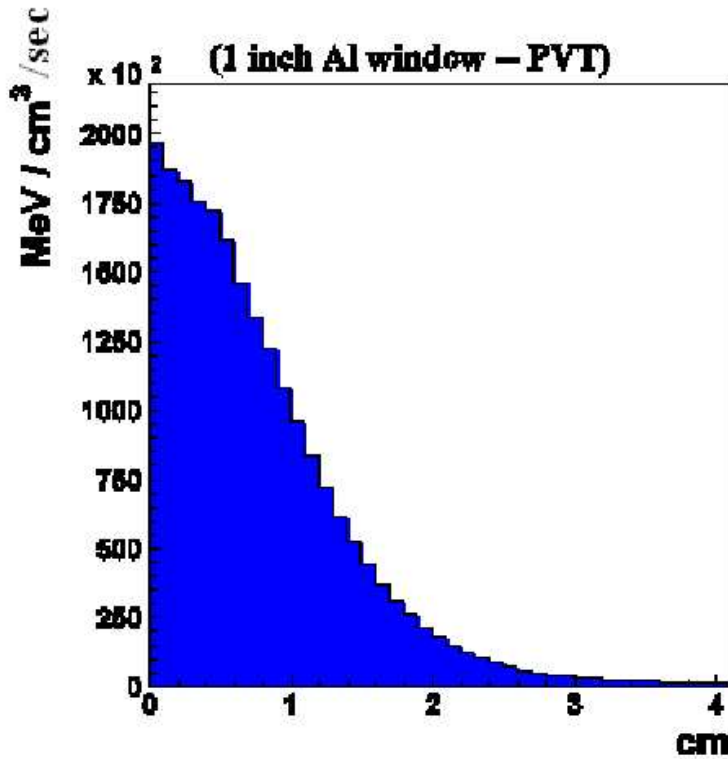


FIG. 2: A GEANT simulation showing a possible photon distribution at the detector.

new voltages to the PMT to increase or decrease the gain factor accordingly when working in new accelerator regimes. Another factor to consider is the time response, which for this photomultiplier tube is 0.78 ns. One of the goals of building the fast luminosity monitor is to have bunch by bunch capability. The beam bunches have frequencies of 14 ns, so this PMT has a fast enough response time for high resolution between beam bunches.

V. GAUSSIAN FITTER

As the window of the detector is 11.05 cm wide and the horizontal divergence of the beam results in a one sigma spot size of 1.05 cm, one can be confident that the window will ‘see’ all of the incoming radiative bhabha photons. However, with a limited vertical length of 5.08 cm, the fast luminosity monitor will not detect all of the photons. In most cases, only a portion of the Gaussian distribution of photons will be observed, yet a complete count is necessary for finding luminosity as Eq. 2 demonstrates. Thus, we must create a program that takes the limited information from the six channels of the detector and finds the parameters to describe a best-fit Gaussian curve.

The equation for a Gaussian distribution is

$$G = \frac{N}{\sigma\sqrt{2\pi}} e^{-(x-\mu)^2/2\sigma^2}, \quad (5)$$

where N is a normalization factor, σ is one standard deviation, and μ is the mean. To find how well our guesses for the three parameters match an ideal Gaussian curve, we calculate

Figure 4: Typical Gain Characteristics

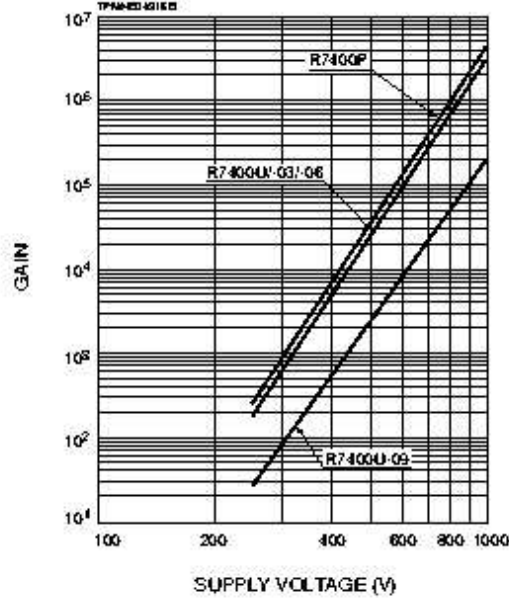


FIG. 3: Graph depicting the operating range of the Hamamatsu R7400U photomultiplier tube used in the fast luminosity monitor.

a value for χ^2 where

$$\chi^2 = \sum_i \frac{(G_2(i) - G_1(i))^2}{\sigma_i^2}. \quad (6)$$

$G_2(i)$ is the theoretical probability distribution that we are testing and $G_1(i)$ is the distribution of actual data points from the fast luminosity monitor [?]. We assume uniform σ_i 's and remove an overall factor of $1/\sigma^2$ from our minimization. By minimizing χ^2 , we find the best-fit Gaussian function under which integration accounts for all photons, whether they struck the monitor or not.

The primary component of the χ^2 minimization program is the Numerical Recipes subroutine *frprmn* [?]. Written in Fortran 90, this routine calls two other subroutines called *func* and *dfunc* both of which we had to provide. *Func* takes in a value for σ , μ , and N and is also provided with the data read from the fast luminosity monitor. It's sole purpose is to calculate χ^2 for those particular parameters. Then, *dfunc* calculates the derivative of χ^2 with respect to σ , μ , and N . This derivative is found numerically by

$$\frac{\partial \chi^2}{\partial P} = \frac{(\chi^2(P + \delta) - \chi^2(P))}{\delta} \quad (7)$$

where P represents one of the three parameters and δ is a small fraction of P .

Using this gradient information, *frprmn* performs consecutive line minimizations to effectively work its way down the gradient. After each iteration, a new value of σ , μ , and N is used as input to *frprmn* and this process continues until χ^2 is sufficiently small. *Frprmn* ultimately finds the 'bottom' of this multi-dimensional bowl representing the values of χ^2 for all three parameters.

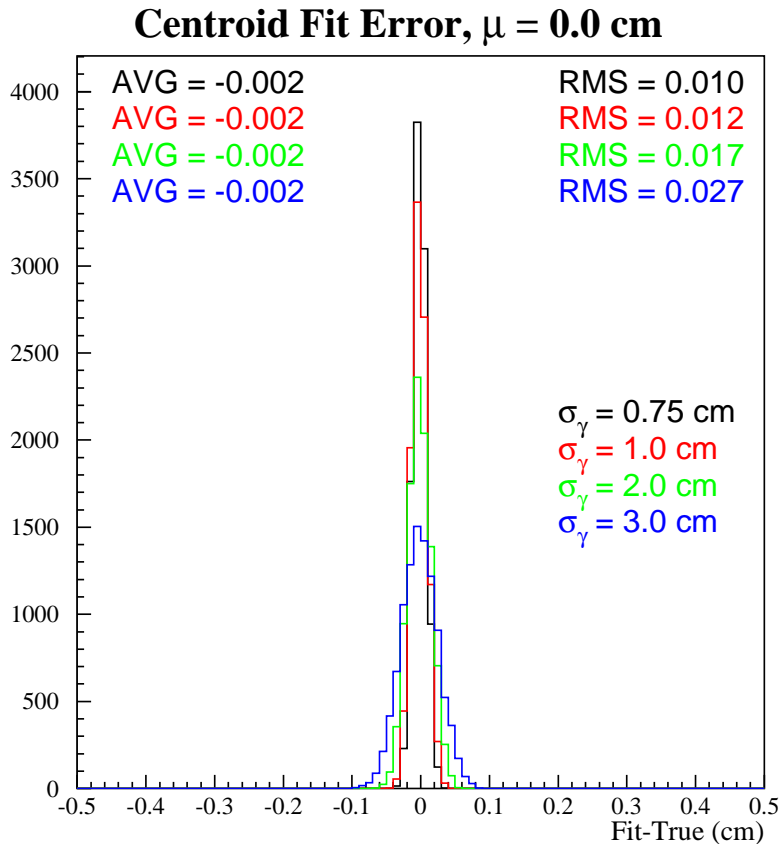


FIG. 4: Histogram plotting the fit-true values for the centroid when $\mu=0.0$ cm without gain error.

A. Data Deviations

Although the ideal situation is that the distribution of radiative bhabha photons at the detector is a perfect Gaussian and all we need do is take the six sample points to determine the shape, this cannot be expected. There will be deviations in the data points with three main sources of error to consider. First, fluctuations in the photon rate will cause a non-perfect Gaussian distribution. However, since we are dealing with rates of magnitude 10^9 photons/sec, deviations approximated by \sqrt{N}/N amount to only 0.003% which can be considered negligible for our purposes of testing the fitter. A second source of deviation arises from electronics noise and here, errors might range from between 0.01% and 1.0%. Third, discrepancies in gain factors from one photomultiplier tube to the next may result in up to 5% deviations from an ideal Gaussian.

These last two scenarios are significant and the fitter must be tested under these conditions. To do so, we wrote a program to generate example data sets with these deviations. For the electronics noise, we set the noise level NL according to

$$NL = \frac{N}{\sigma\sqrt{2\pi}} * \text{perc} \quad (8)$$

where *perc* represents the percentage of deviation. This is then multiplied by a random number that the Numerical Recipes random number generator *gasdev* provides. The result is added to the theoretical data point. To account for gain errors, we implemented the

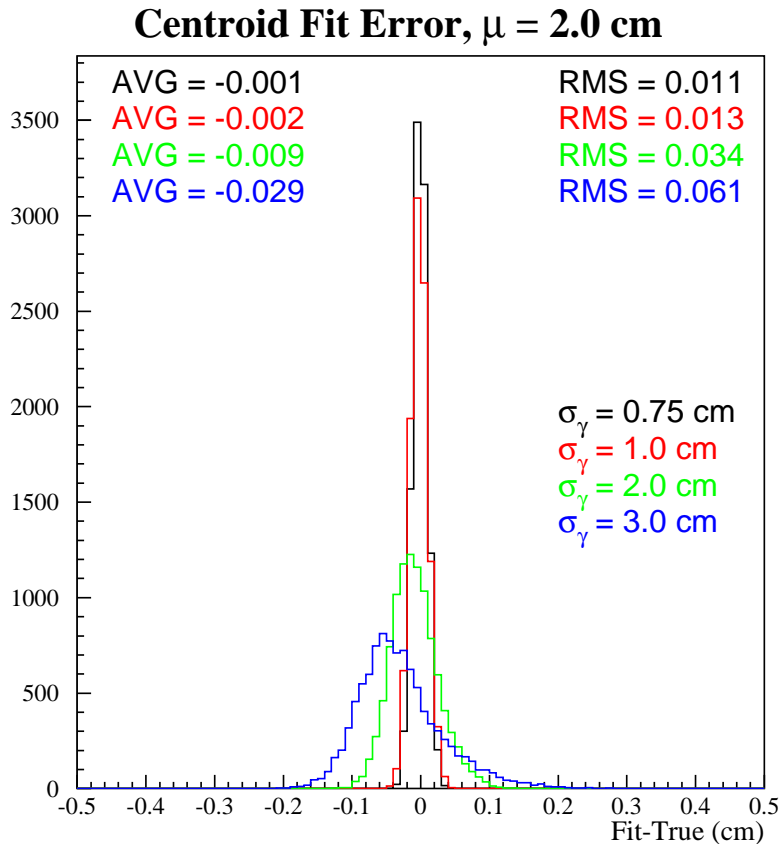


FIG. 5: Histogram plotting the fit-true values for the centroid when $\mu=2.0$ cm without gain error.

random number generator again and multiplied each data point by a gain factor where the root mean square of the sequence of gain factors can be varied.

VI. RESULTS

We test the fitter for both the scenario of electronics noise with no gain factor and the more realistic scenario which includes noise and gain errors. We use twelve different combinations of photon beam position and divergence. Values for the centroid of the beam, μ , range from 0.0 to 2.0 cm and the divergence, σ_γ , ranges from 0.75 to 3.0 cm. The six scintillators are placed at -2.75, -1.65, -0.55, 0.55, 1.65, and 2.75 cm from the center of the window. We ran the fitter 10,000 times for each combination of μ and σ_γ , letting the random number generator use different numbers each time. A constant value of $N=1$ was used. For all data presented here, the root mean square of the gain factor is 4.6% and the noise error is 1.0%.

Figure 4 is a histogram depicting how well the fitter program could find the centroid of the beam. When the beam is such that $\mu=0.0$, the center is found to always be within 2.0 mm of the actual value no matter what the divergence is. When the beam is offset (see Fig. 5) by 2 cm, the fitter still works very well, only ever underestimating the centroid by at most 3.0 mm for $\sigma_\gamma=3.0$. For an electronics noise of 1%, the fact that the precision is at the 1.0 mm level is very good as that is the best that we can hope for. With gain errors, the centroid is still found with very high accuracy and a precision on the order of a tenth of

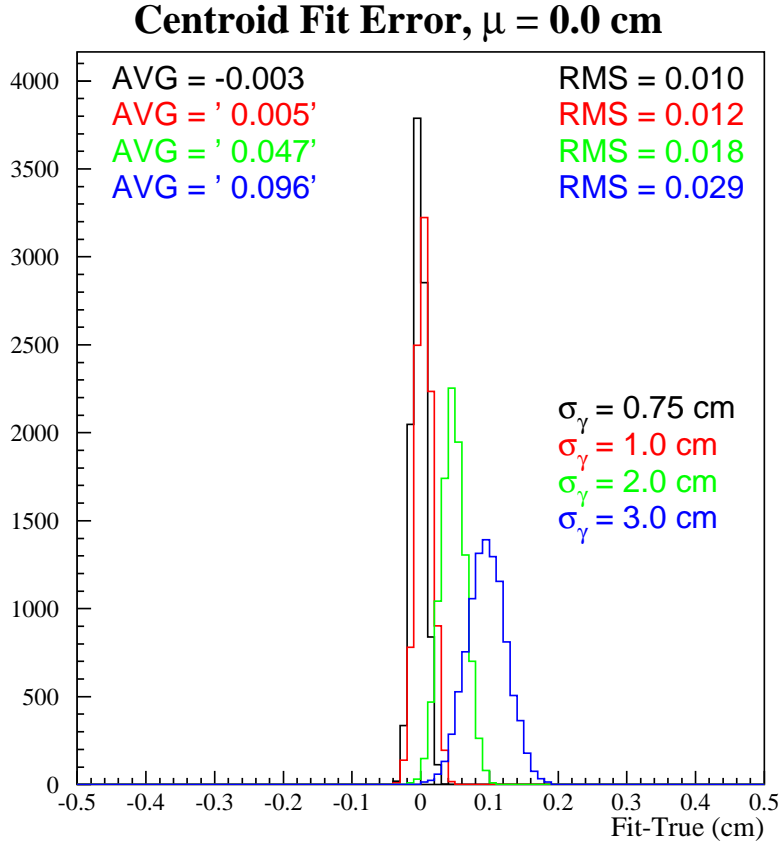


FIG. 6: Histogram plotting the fit-true values for the centroid when $\mu=0.0$ cm with gain error.

a millimeter as shown in Figures 6 and 7. This even holds true for the worst case scenario when the beam is widely spread out and displaced 2 cm from the center of the monitor.

As the purpose of the fast luminosity monitor is to count the number of photons and then relate that to a value for luminosity, how well the fitter finds the correct value of the normalization constant N is very important. We see in Fig. 8 and 9 where the histograms show fractional errors, that there is at most a 1.0% difference between real and fitted values. The uncertainties are all around 1.5%, again consistent with the 1% electronics noise added on. Including gain errors to each channel provides more interesting results as offhand, we see how the fitter overestimates the rate when the beam is centered (See Fig. 10) and the fitter underestimates the rate when the beam is displaced 2 cm (See Fig. 11). When $\sigma_\gamma=0.75$ cm, there is a spread of 5% in the accuracy of finding the rate. For such a narrow Gaussian distribution, most of the data is concentrated in one channel, so the particular gain factor plays a larger role than with the wider beams. Despite this effect, we are still finding the rate with a high precision on the order of 1%.

The fractional fit error for the third parameter, divergence of the photon beam, is shown in Figures 12-15. Given no gain errors, the divergence is found to within a fraction of a percent. We see that the fitter is slightly less accurate and precise when it has to fit to the wider beam of $\sigma_\gamma=3.0$ cm, but this has at most a 1.0% deviation from the actual value with a 1.9% uncertainty for the case when $\mu=2.0$ cm. When $\sigma_\gamma=1.0$ cm, the average percent error is 0.3%. Interesting effects are seen upon adding in gain errors. As the beam is shifted from the center to an offset of 2.0 cm on the window, the effects of the specific gains for

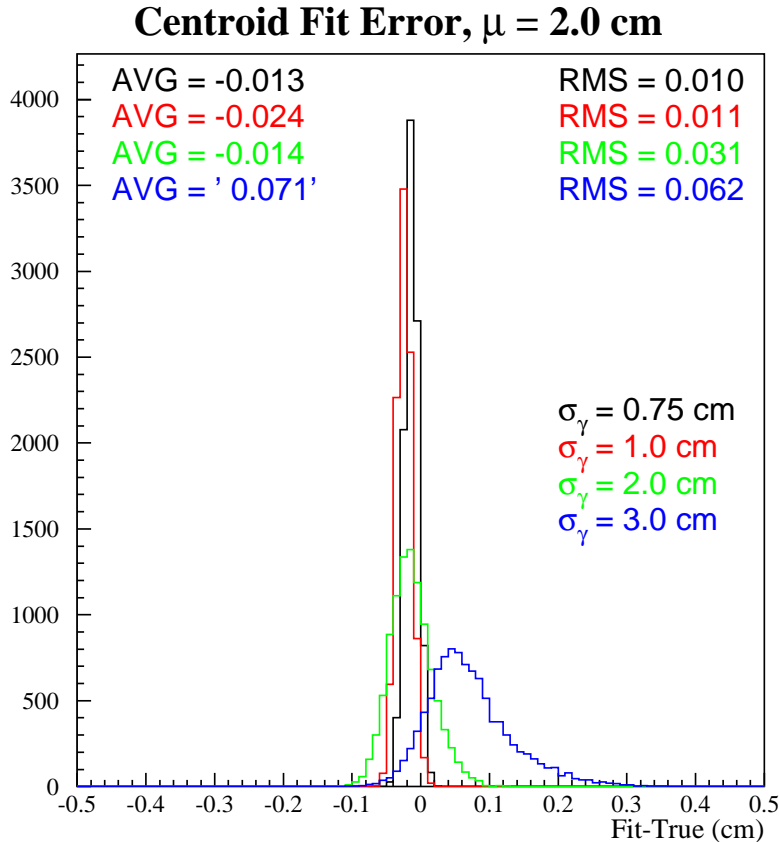


FIG. 7: Histogram plotting the fit-true values for the centroid when $\mu=2.0$ cm with gain error.

each channel are seen. For all cases of divergence when the centroid is at $\mu=0$, the accuracy is at the worst a 2.7% overestimate. We see this change to at worst a 5.8% underestimate when $\mu=2.0$ cm. However, the precision does not vary much and it ranges from 1.0 to 1.9%.

VII. CONCLUSIONS

Testing Gaussian fitter and its χ^2 minimization subroutine for various situations of expected photon beam divergence and centering on the detector proves the algorithm works well. Given that the beam will have a typical divergence of 1 to 2 cm, we tested these two values as well as extrema on either side for a perfectly centered beam and a beam displaced 2 cm in the 5.08 cm length window. Electronics noise and gain errors to account for discrepancies from one photomultiplier tube to the next were added to prototype data.

The fitter always finds the centroid of the beam to within 0.2 mm of the actual center and with a high precision of 0.1-0.2 mm. Thus, the CESR operator will be able to easily detect when the beam becomes misaligned and can bring it back to the center. However, it is important to note that even when not centered and with gain errors, the fitter finds the rate of photons with only at most a 2.9% error when $\sigma_\gamma=0.75$ cm. This error is merely 0.5% with the more likely case of $\sigma_\gamma = 1.0$ cm.

Systematic biases creep in with gain errors especially when the beam is very narrow. This is seen in determining the rate where the percent error jumps from -2.3% to 2.9% for $\mu=0$ to 2 cm. The high discrepancies that these gain errors cause from one data set to the next

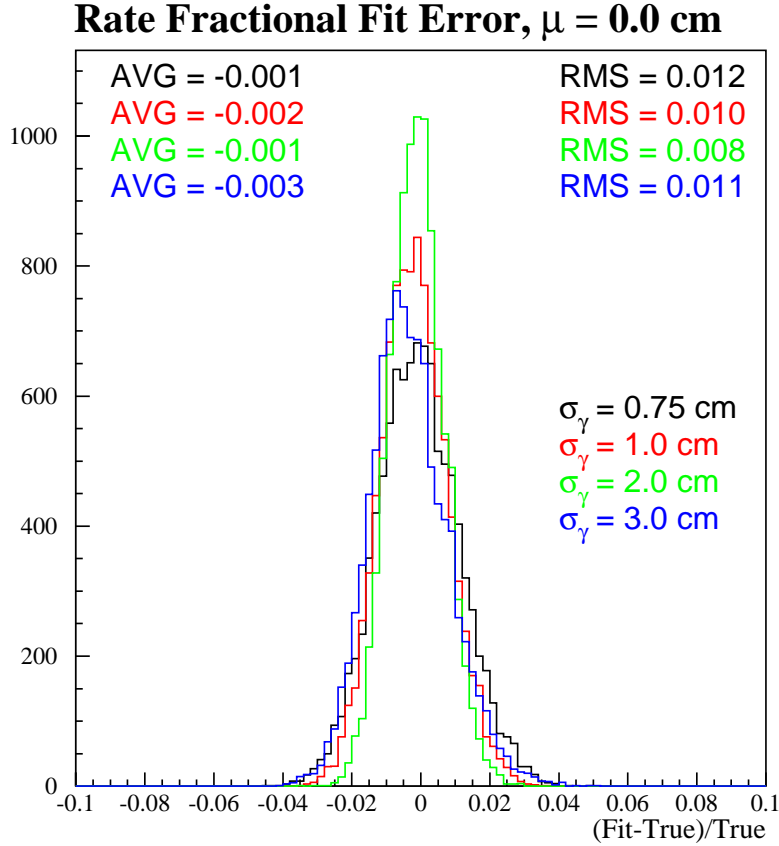


FIG. 8: Histogram plotting the fractional errors for the rate when $\mu=0.0$ cm without gain error.

set the level at which we must calibrate the readout channels. Without a careful calibration of these gains, we can expect a several percent systematic offset in determining the photon beam divergence among the other parameters.

Thus, with the limitations of one piece of data from each of the six scintillators, and a fast luminosity monitor window of 5.08 cm in the vertical direction which is not large enough to count all incoming radiative bhabha photons, we have nonetheless created a program to find the luminosity at the interaction point. This luminosity is only a relative value, but absolute calibration takes place using CLEO Barrel measurements. However, the fitter fails every 1/10,000 times. With an update rate of 1 Hz, this corresponds to an average of one failure every few hours.

Future work to improve the code constitutes optimizing a delta finding routine. While numerically calculating the gradient of χ^2 , deltas for each of the parameters must be determined. Currently, the fitter uses a preset value which might not provide the most accurate result or which might be more precise than is necessary, using extra computing time. Furthermore, altering some of the structure of the code so that one can easily include more parameters would be ideal. Last, as installation of the fast luminosity monitor will begin within this next week, creating the interface between the Gaussian fitter program and the CESR control system computers is the next most important step to take.

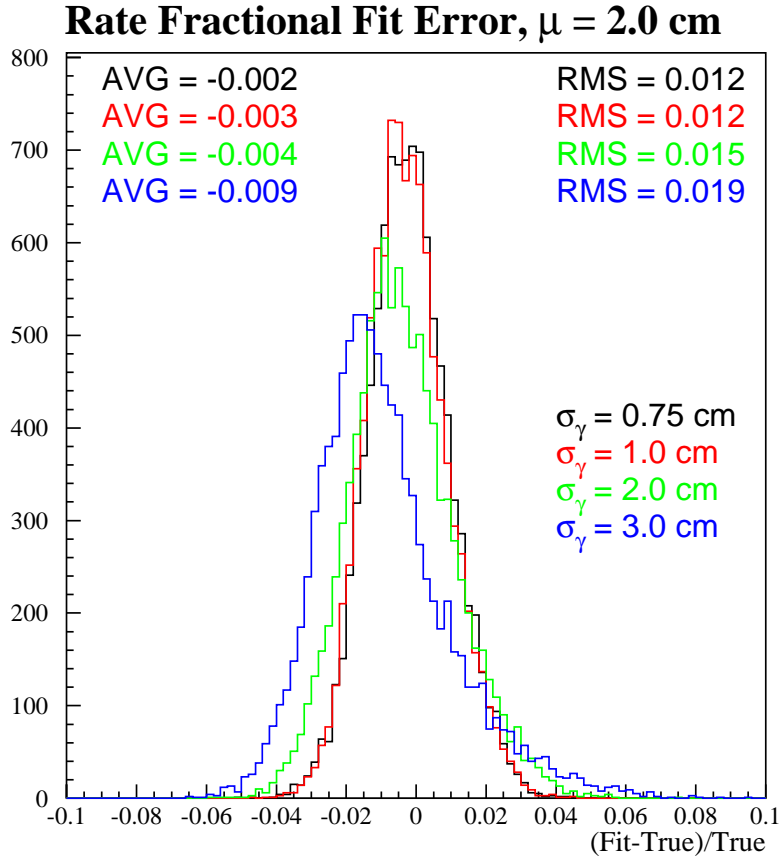


FIG. 9: Histogram plotting the fractional errors for the rate when $\mu=2.0$ cm without gain error.

VIII. ACKNOWLEDGMENTS

I would like to thank Mark Palmer, of Cornell University, who created and guided me through this project. I appreciate all of the time he spent with me to explain concepts and help debug code. I also thank Rich Galik for overseeing this Research Experience for Undergraduates program and all of my fellow REU LEPPers for their support and friendships. This work was supported by the National Science Foundation REU grant PHY-0243687 and research co-operative agreement PHY-9809799.

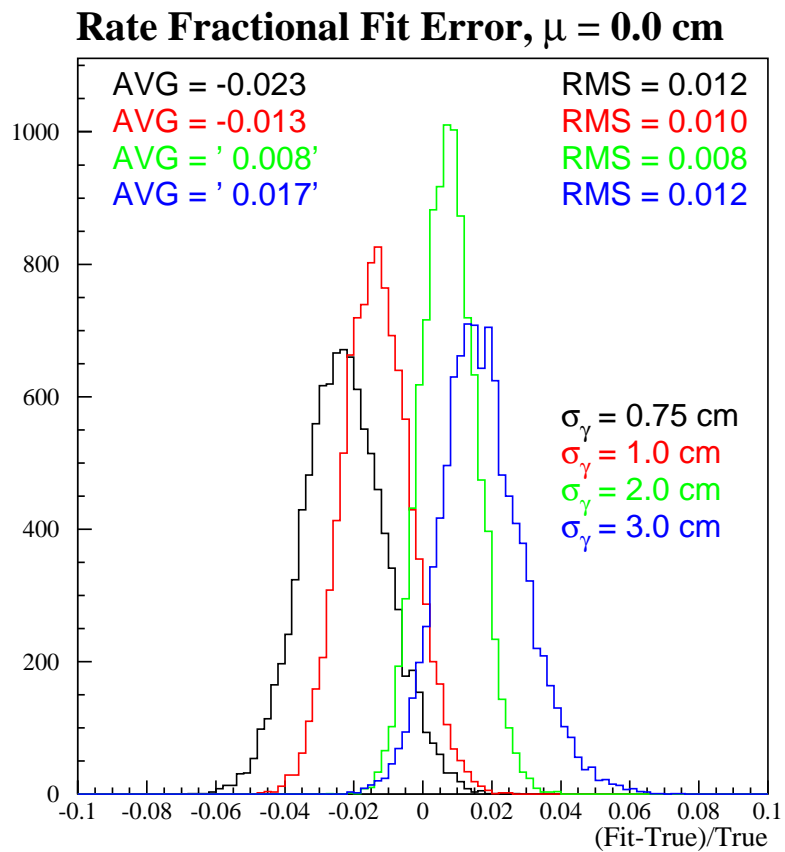


FIG. 10: Histogram plotting the fractional errors for the rate when $\mu=0.0$ cm with gain error.

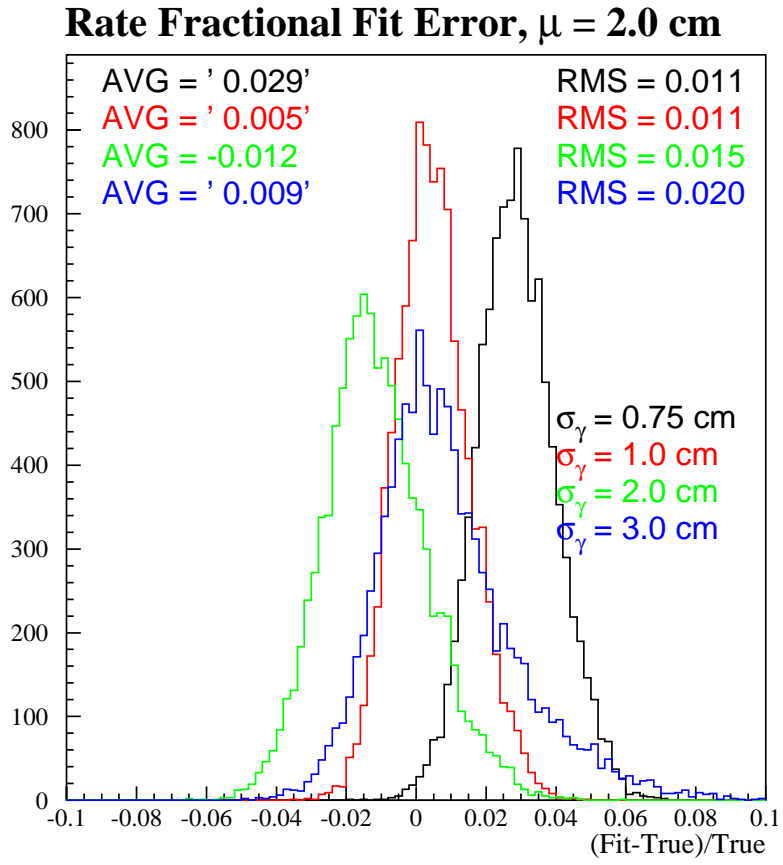


FIG. 11: Histogram plotting the fractional errors for the rate when $\mu=2.0$ cm with gain error.

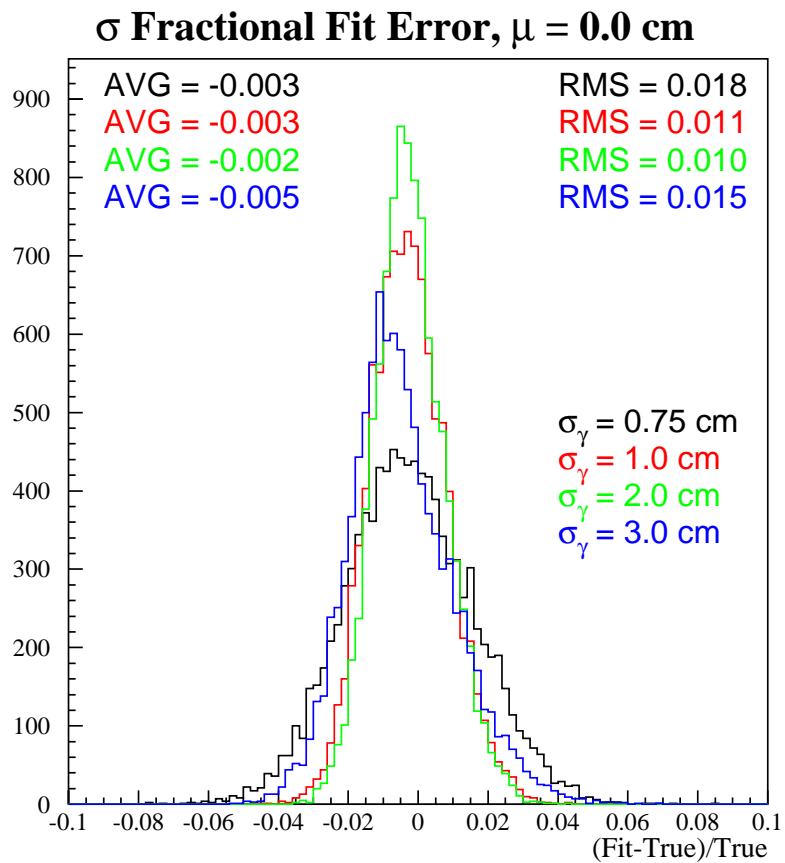


FIG. 12: Histogram plotting the fractional errors for the divergence when $\mu=0.0$ cm without gain error.

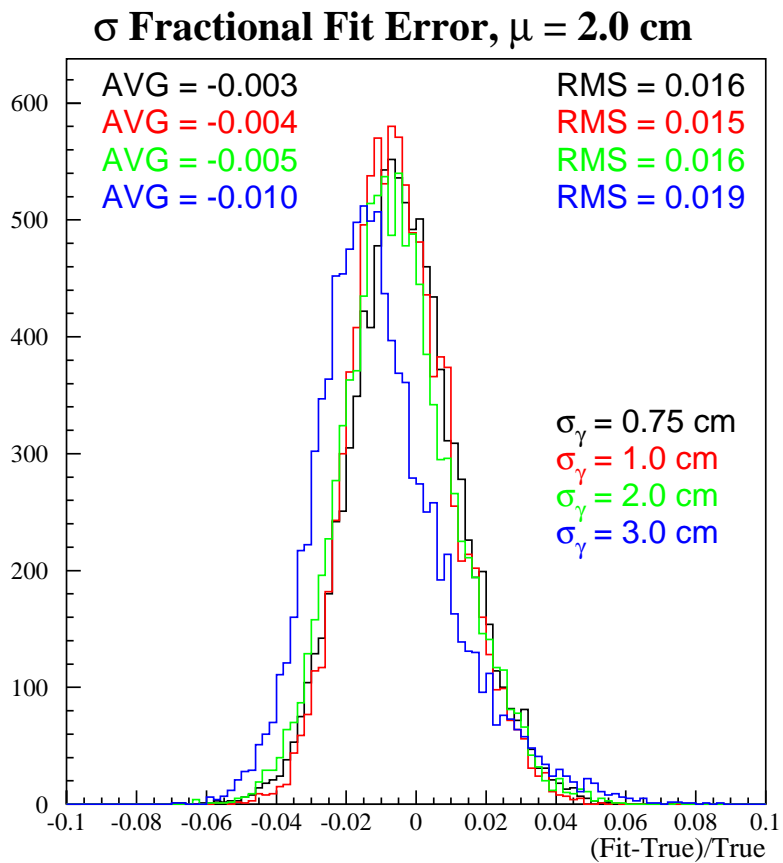


FIG. 13: Histogram plotting the fractional errors for the divergence when $\mu=2.0$ cm without gain error.

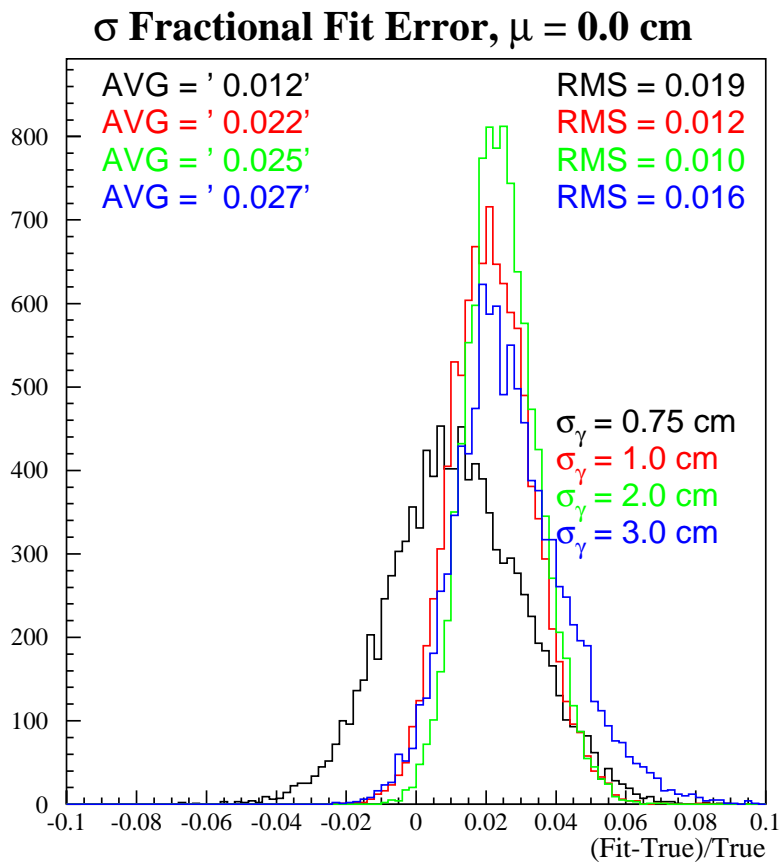


FIG. 14: Histogram plotting the fractional errors for the divergence when $\mu=0.0$ cm with gain error.

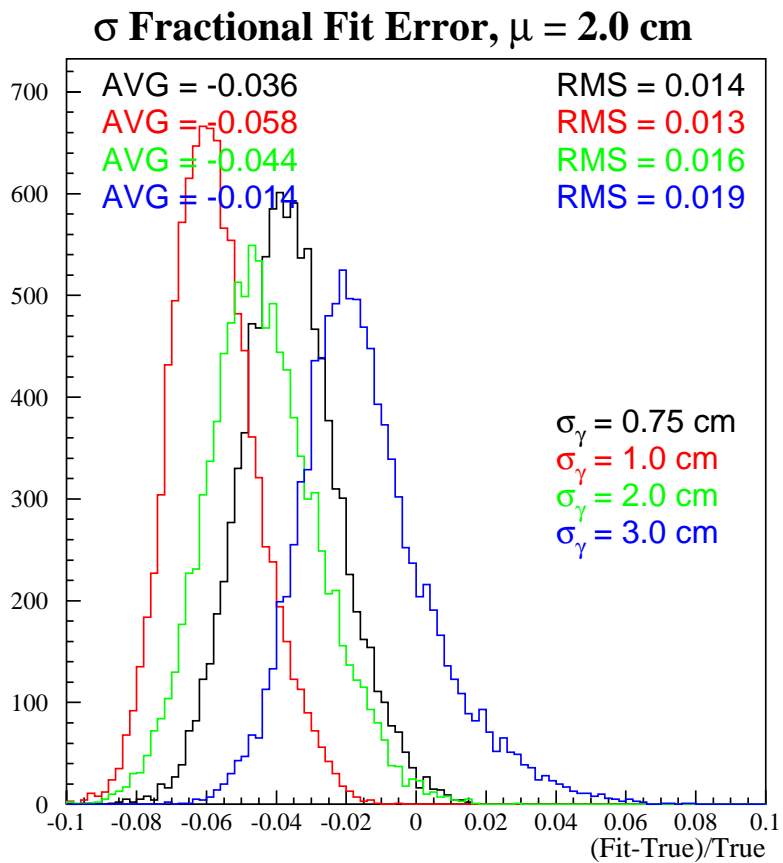


FIG. 15: Histogram plotting the fractional errors for the divergence when $\mu=2.0$ cm with gain error.